

# Two measures elaborated for entangled states: Quantum entropy and fidelity using Schmidt coefficients of the reduced density matrix of full TRI

R. Dermez<sup>a,b,c</sup> and Y. Tunçer<sup>d</sup>

<sup>a</sup>*Department of Physics, Afyon Kocatepe University, Afyonkarahisar, 03200 Turkey.  
email: dermez@aku.edu.tr*

<sup>2</sup>*Department of Electrical and Computer Engineering,  
Michigan Technological University, Michigan, 49931, USA.*

<sup>c</sup>*Afyon Vocational School, Afyonkarahisar, 03200, Turkey.*

<sup>d</sup>*Mathematics Department, Faculty of Science, Usak University, Usak, Turkey.*

Received 24 October 2021; accepted 27 December 2021

In the present study, we determined quantum entanglement in a full trapped ion (TRI)-coherent system and its dependence on the Lamb-Dicke parameter (LDP). We investigated the entanglement in view of two elaborated measurements of the family: entropy and fidelity. We selected three values of the deep LDP to demonstrate the benefits of these two critical measures. The findings obtained in this study showed that the maximum value of fidelity for entangled states is quantified approximately to be 0.35, and the long lifetime is also observed with entropy measurement. The findings suggest that three coupling parameters play a significant role in developing quantum entanglement.

*Keywords:* Qudit states; fidelity; the total density operator; quantum correlations.

DOI: <https://doi.org/10.31349/RevMexFis.68.050703>

## 1. Introduction

A few months after the Einstein-Podolsky-Rosen [1] article was published in 1935, in the same year, articles were published in reaction by Erwin Schrödinger [2] and Niels Bohr [3]. Schrödinger coined the word "entanglement" to describe a condition in this famous EPR paper. The discussion of these three papers focuses on describing two entangled particle states and the characterization of the quantum correlations between them. The entanglement of two-qubits, two-qutrits or the two-quadrants is quantum-mechanically interesting. Correlation in an entangled system cannot be explained using classical correlations [4]. Quantum entanglement has been proposed as a proof of quantum correlations [2].

The study of quantum entanglement has advanced over the past years due to the further development of quantum physics [5–7]. Entangled states can be worked in different physical setups, such as massive particles like TRIs [5]. Entanglement between electronic levels of the TRI has been an active field of study in recent years [6]. The high-fidelity entanglement between a TRI and a photon is measured by quantum frequency conversion [7].

In this context, qudits are used as higher capacity quantum information sources, and could be of interest for quantum communication [8]. The higher dimension of a given Hilbert space, the more quantum correlation continuity is ensured. A quantum dit (qudit) is the unit of quantum information described by a superposition of "d" states, where the number of states is an integer greater than two. For example, qutrit or quadrant state can be called a qudit state. Pure and mixed qudits can be obtained due to the interaction between two laser beams and the three-levels TRI with specific initial

state conditions [6, 9, 10]. It is fundamental within the probability interpretation as initiated by M. Born and pushed into a general form by P. A. M. Dirac, J. von Neumann, G. Birkhoff and many others [11].

Fidelity (Transition Probability) for pairs of density matrices can be defined as a tool in the hierarchy of all quantum systems. Uhlmann and Jozsa's papers are considered classic fidelity studies [12–14]. Fidelity, negativity, purity, and concurrence are popular methods for quantum entanglement [15–17]. A structure worthy of study is presented in Ref. [18] for multiplexed quantum repeaters that use local connectivity to improve accuracy in entanglement distribution.

The existence of atomic motion, which becomes most obvious for the high-dimensional Hilbert space of pure qudit states is shown in [19]. A two-level atom and a two-level ion, and a photon with spin up-spin down probability are associated with two-dimensional Hilbert space. In general, the n-level atom and the n-level ion are defined as the n-dimensional Hilbert space. Interaction of an atom or an ion with a photon is associated with a higher-dimensional Hilbert space in the tensorial product such as ( $H = H_1 \otimes H_2$ ). We expand the physical model that has been improved before for studying Schrödinger cat states of the two phonons [20]. The n-dimensional Hilbert space in Ref. [20] is restricted to 12 dimensions in this study. This limitation has led to easy analytical results. Characterization of the quantum entanglement can be explored using entropy [21] and fidelity [22–24], which apply to the bipartite systems of arbitrary dimensions in TRIs. Hence this situation fits our purposes. By means of quantum entropy, it is shown whether the entanglement lifetime is extended or not [21]. There are both contributions and

compatibilities between Ref. [25]'s fidelity calculations and this paper.

The outline of this study is as follows. The theoretical framework of the qutrit-quadrid in the physical system is introduced in Sec. 2. the quantum entropy and the fidelity are discussed with corresponding Figures in Sec. 3. Finally, we give the results of the quantum measure in Sec. 4.

## 2. Evaluation of qutrit-quadrid in the physical system

We focus a TRI in a harmonic potential and two coherent states (or two photons). Also, we develop a new physical system based on the quantum system mentioned in [20]. The concept of the time evolution of the physical model is introduced using the density matrix, which affects the state necessary for quantum dynamics in [26]. The harmonic trap frequency is designed to construct a linear trap so that the TRI's center-of-mass (c.m.) motion is effectively one dimensional along the  $x$  axis. Therefore, we consider small vibrations of a TRI in the harmonic trap which can be defined as coherent displacements. The quantum state of the TRI's c.m. motion is characterized by a coherent state  $|\alpha\rangle$  with  $\alpha \ll 1$  in this way. For the first order in  $\alpha$ , this describes as a qubit of two phonons  $|0\rangle + \alpha|1\rangle$ .

The physical system is assumed to interact with two coherent states in a  $\Lambda$  scheme with the mass of the TRI  $m$  and the linear harmonic trap frequency  $\nu$ . A total Hamiltonian is determined in the  $\Lambda$  configuration for optical transitions. The total Hamiltonian of the TRI-coherent system is  $H_{total} = H_{ion} + H_{e-g} + H_{e-r}$ , and  $H_{ion}$  is called the Hamiltonian of the TRI. The  $H_{ion}$  is given as the following:

$$H_{ion} = \frac{p_x^2}{2m} + \frac{1}{2}m\nu^2 x_{ion}^2 - \delta_1 |e\rangle\langle e| - (\delta_1 - \delta_2) |r\rangle\langle r|.$$

$$H_{ion} = \frac{p_x^2}{2m} + \frac{1}{2}m\nu^2 x_{ion}^2 - \delta_1 |e\rangle\langle e| - 0 |r\rangle\langle r|. \quad (1)$$

The assumptions and the parameters used in the TRI-coherent system are given as follows:  $\delta_1 = \omega_1 - \omega_{eg}$  and  $\delta_2 = \omega_2 - \omega_{er}$ .  $\omega_{eg}$  is the resonance frequency of e-g transition and  $\omega_{er}$  is the resonance frequency of e-r transition. The frequencies of the two photons are equal to  $\omega = \omega_1 = \omega_2$  (See Fig. 1). Here  $p_x$  is the momentum operator and  $x_{ion}$  is the x-component of the position operator using the Planck constant equal to one, ( $\hbar = 1$ ). The TRI c.m. motion is described by the standard harmonic-oscillator quantization of  $H_{ion}$  [20] via  $p_x = -i\sqrt{(1/2)m\nu}(a^\dagger - a)$  and  $x_{ion} = \sqrt{(1/2m\nu)}(a^\dagger + a)$ . Bosonic operators  $a$  and  $a^\dagger$  according the usual Weyl-Heisenberg algebra are the annihilation and the creation of the phonons.

We consider the lower levels  $g$  and  $r$  to be degenerate. Therefore, the energy of the ground level is equal to the Raman energy  $\omega_r = \omega_g = 0$ , the excited energy and is  $\omega_e$ . We focus on a nontrivial quantum case of a weakly detuned our system in which  $\Delta = \delta_1 - \delta_2 = 0$  and  $\delta_1 = -\nu\eta^2$ .  $\Delta = 0$

can be true when lower levels of the ion are degenerate in Eq. (1). The Lamb-Dicke parameter (LDP) is  $\eta = k/\sqrt{2m\nu}$ . The wavevectors  $k_1$  and  $k_2$  characterize the two photons with  $k = k_1 = k_2$ , and  $k = 2\pi/\lambda$ . The wavelength of both photon  $\lambda$  is red detuned from the upper level  $e$  by the same amount  $\delta_1 = \delta_2 = -\nu\eta^2$ . If the frequencies and wavevectors of the two incoming photons do not take as equal ( $\omega_1 \neq \omega_2$ ;  $k_1 \neq k_2$ ), then  $\Delta \neq 0$ , that is,  $r$  and  $g$  levels can not be degenerate. So that,  $|r\rangle\langle r|$  can be visible in Eq. (1) and Eq. (4).

$H_{e-g}$  and  $H_{e-r}$  are the interaction Hamiltonians between these levels  $e-g$  and  $e-r$  using  $\hbar = 1$ . The interaction Hamiltonians are defined as follows:

$$H_{e-g} = \frac{\Omega}{2} e^{i(k_1 x_{ion} - \omega t)} |e\rangle\langle g| + h.c., \quad (2)$$

$$H_{e-r} = \frac{\Omega}{2} e^{i(-k_2 x_{ion} - \omega t)} |e\rangle\langle r| + h.c. \quad (3)$$

here, atomic levels of the TRI are given, such as  $|g\rangle \rightarrow$  TRI-ground level,  $|r\rangle \rightarrow$  Raman level and  $|e\rangle \rightarrow$  excited level (See Fig. 1). The Rabi frequencies of the dipole interactions between the photons and the TRI's are given by  $\Omega$  in Eq. (2) and Eq. (3). So that, the equality of Rabi frequencies is taken by  $\Omega = \Omega_1 = \Omega_2$ . In this approach, the mathematical equations are obtained by  $\delta_1 = \delta_2$  and  $\Omega_1 = \Omega_2$ .

We now remove the Bose variables from the interaction part of the Hamiltonian in Eq. (2) and Eq. (3). Thus, the exponential expressions have some variations. Because of the degeneracy,  $\Delta = 0$  and the two exponential expressions are as follows:  $e^{i(k_1 x_{ion} - \omega t)} = e^{i\eta(a^\dagger + a)}$  and  $e^{i(-k_2 x_{ion} - \omega t)} = e^{-i\eta(a^\dagger + a)}$ . Therefore, the total Hamiltonian is rewritten as

$$H = \left( \frac{\Omega}{2} e^{i\eta(a^\dagger + a)} |e\rangle\langle g| + \nu a^\dagger a - \delta |e\rangle\langle e| - 0 \right. \\ \left. + \frac{\Omega}{2} e^{-i\eta(a^\dagger + a)} |e\rangle\langle r| \right) + h.c., \quad (4)$$

with respect to the base vectors as the following:

$$|e\rangle = \begin{pmatrix} 1 \\ 0 \\ 0 \end{pmatrix}, \quad |r\rangle = \begin{pmatrix} 0 \\ 1 \\ 0 \end{pmatrix}, \quad |g\rangle = \begin{pmatrix} 0 \\ 0 \\ 1 \end{pmatrix}. \quad (5)$$

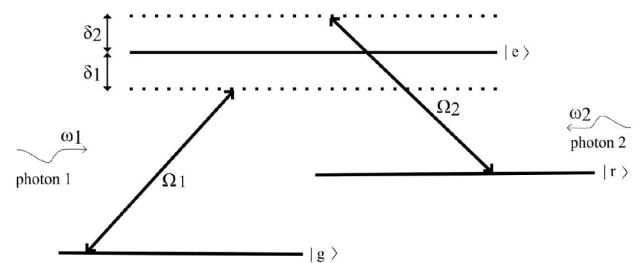


FIGURE 1. Three internal electronic levels of the TRI interacting with two photons in the  $\Lambda$  configuration. The coupling parameters of the system are assumed as  $\Omega = \Omega_1 = \Omega_2$ ,  $\omega = \omega_1 = \omega_2$ , and  $\delta = \delta_1 = \delta_2$ .

$\tilde{H} = U^\dagger H U$  is the transformed Hamiltonian. The Hamiltonian in Eq. (4) turns into the Hamiltonians of Eqs. (7-8)

with the transformation process. In this transformation we used the most extended weak excitation regime. The weak excitation regime is applied by  $\Omega = 2\nu$ . With this mathematical approach, this optical  $\Lambda$  configuration demonstrated to be equivalent to a cascade configuration for the phonon transition, under the unitary transformation [20]. The TRI-coherent system evolves in the optical  $\Lambda$  configuration. The transformation matrix  $U$  is defined as [20]:

$$U = \frac{1}{2} \begin{pmatrix} 0 & \sqrt{2} & \sqrt{2} \\ -\sqrt{2}B[\eta] & B[\eta] & -B[\eta] \\ \sqrt{2}B[-\eta] & B[-\eta] & -B[-\eta] \end{pmatrix}. \quad (6)$$

Here, Glauber displacement operators are represented by  $B(\pm\eta) = e^{\pm(i\eta(a+a^\dagger))}$ . The transformed Hamiltonian,  $\tilde{H}$  is described with cascade-type transitions of the two phonons, under a rotating wave approximation (RWA). The RWA is valid for  $\eta < 1/\alpha$ , where  $\alpha$  characterizes the amplitude of coherent displacement of the phonons [20]. The RWA and the transformation method in Eq. (6) allow for working effects of larger  $\eta$ , for example, the third value of  $\eta$  (See Figs. 2, 3 and 4). After this transformation operation,  $\tilde{H}$  is written as  $\tilde{H} = \tilde{H}_0 + \tilde{V}$ , where

$$\tilde{H}_0 = \nu(|r\rangle\langle r| - |g\rangle\langle g|) + \nu\eta^2 + \nu a^\dagger a, \quad (7)$$

and

$$\tilde{V} = -i\frac{\sqrt{2}\delta\eta}{2} (a^\dagger|e\rangle\langle r| - a^\dagger|e\rangle\langle g| + h.c.). \quad (8)$$

Under the unitary transformation method [20], the time evolution of an early position  $\psi(0)$  is defined as follows:

$$\begin{aligned} |\psi(t)\rangle &= U_0^\dagger U e^{-it\tilde{H}_0} K(t) U^\dagger |\psi(0)\rangle \\ &= U_0^\dagger U e^{-it\tilde{H}_0} K(t) |\psi_K(t)\rangle, \end{aligned} \quad (9)$$

where  $K(t)$  is the propagator vector and  $e^{(-it\tilde{H}_0)}$  is term of the interaction picture transformation. The two rightmost factors  $U^\dagger |\psi(0)\rangle = |\psi_K(t)\rangle$  act as the early state for the cascade system, evolving  $K(t)$  into  $|\psi_K(t)\rangle$ . The rotating frame transformation is given by the prefactor matrix  $U_0 = \exp(-i\omega t|e\rangle\langle e|)$  [20]. The propagator is obtained as

$$K(t) = \frac{1}{2} \begin{pmatrix} \text{Cos}(\Lambda t) & -\epsilon S a^\dagger & -\epsilon S a \\ \epsilon a S & 1 + \epsilon^2 a G a^\dagger & \epsilon^2 a G a \\ \epsilon a^\dagger S & \epsilon^2 a^\dagger G a^\dagger & 1 + \epsilon^2 a^\dagger G a \end{pmatrix}, \quad (10)$$

here  $\epsilon = \nu\eta/\sqrt{2}$ ,  $\Lambda = \epsilon\sqrt{2a^\dagger a + 1}$ ,  $G = \text{Cos}(\Lambda t) - 1/\Lambda^2$ , and  $S = \text{Sin}(\Lambda t)/\Lambda$ . The trap frequency of the system is taken by  $\nu = 10^4$  Hz. Because the most suitable mathematical values for the systems are the trap frequencies between  $10^3$  and  $10^6$  Hz. Under all approaches and transformations, the new general formula of the system is given as

$$\begin{aligned} |\psi(0)\rangle &= \left[ \frac{1}{\sqrt{3}}|g\rangle + \frac{1}{\sqrt{3}}|r\rangle + \frac{1}{\sqrt{3}}|e\rangle \right] \\ &\otimes \left( \sum_{n=0}^{\infty} F_n(b)|n\rangle \right). \end{aligned} \quad (11)$$

The initial state of the TRI-coherent system is defined as

$$|\psi(0)\rangle = \frac{1}{\sqrt{3}}[|g\rangle + |r\rangle + |e\rangle] \otimes (b|0\rangle + \alpha|1\rangle), \quad (12)$$

here, the matrix representations of the coherent states are  $\langle 0| = (1, 0)$ , and  $\langle 1| = (0, 1)$ . The generalized coherent state is  $F_n(\alpha) = e^{-|\alpha|^2/2}(\alpha^n/\sqrt{n!})$  in Eq. (11).  $n = 0$  and  $n = 1$ ,  $F_0 = b$  and  $F_1 = \alpha$  are the amplitudes of the Fock number states of two phonons. The probability amplitudes of the coherent states are given as  $b = 1$  and  $\alpha = 0.005$ . The TRI normalization condition is exactly  $[1/\sqrt{3}]^2 + [1/\sqrt{3}]^2 + [1/\sqrt{3}]^2 = 1$ , and two phonons normalization condition is approximately  $\|b\|^2 + \|\alpha\|^2 = |1|^2 + |0.005|^2 \simeq 1$ . We have shown the TRI-coherent system as  $l \otimes l'$  in Eqs. (11-12). Considering Eq. (12), the dimensionality of the Hilbert space is defined as: The Hilbert space dimensions are  $l = 4$  for the two-phonons and  $l' = 3$  for the full TRI. The TRI-coherent system is in Hilbert 12-space. For the two rightmost terms of Eq. (9), the TRI-coherent state is transformed into an early case of the cascade

$$|\psi_K(t)\rangle = U^\dagger |\psi(0)\rangle = \sum_{\sigma, m} M_{\sigma, m}(t) |\sigma, m\rangle. \quad (13)$$

Because of the transformation matrix, Eq. (12) is produced by  $\sum_{\sigma, m} M_{\sigma, m}(t) |\sigma, m\rangle$  in the system. The twelve probability amplitudes belong to the TRI-coherent system are given as

$$M_{e0}(t) = \left[ \sqrt{\frac{2}{3}} \cos(\sqrt{0.5}t) - \frac{1}{\sqrt{6}} \sin(\sqrt{0.5}t)\alpha + \frac{i\eta}{\sqrt{3}} \sin\sqrt{0.5}t \right] \exp[-it\eta], \quad (14)$$

$$M_{e1}(t) = \left[ -\frac{1}{\sqrt{18}} \sin\left(\sqrt{\frac{3}{2}}t\right) + \sqrt{\frac{2}{3}}\alpha \cos\left(\sqrt{\frac{3}{2}}t\right) \right] \exp\left[\frac{-it}{\eta}\right], \quad (15)$$

$$M_{e2}(t) = \left[ -\frac{\alpha}{\sqrt{15}} \sin\left(\sqrt{\frac{5}{2}}t\right) - i\eta\sqrt{\frac{2}{15}} \sin\left(\sqrt{\frac{5}{2}}t\right) \right] \exp\left[\frac{-2it}{\eta}\right], \quad (16)$$

$$M_{r0}(t) = \left[ \alpha \sqrt{\frac{2}{3}} \sin \left( \sqrt{\frac{3}{2}} t \right) + \frac{2}{\sqrt{54}} + \frac{1}{\sqrt{54}} \cos \left( \sqrt{\frac{3}{2}} t \right) \right] \exp \left[ \frac{-it}{\eta} \right], \quad (17)$$

$$M_{r1}(t) = \left[ \alpha \left( \frac{3}{\sqrt{150}} + \frac{2}{\sqrt{150}} \cos \left( \sqrt{\frac{5}{2}} t \right) \right) + i \left( \frac{3 + 2 \cos \left( \sqrt{\frac{5}{2}} t \right)}{\sqrt{75}} \right) \eta \right] \exp \left[ \frac{-2it}{\eta} \right], \quad (18)$$

$$M_{g0}(t) = \frac{1}{\sqrt{6}} \exp[-it\eta] \quad (19)$$

$$M_{g1}(t) = \left[ \alpha \frac{1}{\sqrt{6}} \cos \left( \sqrt{\frac{1}{2}} t \right) + \sqrt{\frac{2}{3}} \sin \left( \sqrt{\frac{1}{2}} t \right) - \frac{i\eta}{\sqrt{3}} \cos \left( \sqrt{\frac{1}{2}} t \right) \right] \exp[-it\eta] \quad (20)$$

$$M_{g2}(t) = \left[ -\frac{1}{\sqrt{27}} + \frac{1}{\sqrt{27}} \cos \left( \sqrt{\frac{3}{2}} t \right) + \alpha \frac{2}{3} \sin \left( \sqrt{\frac{3}{2}} t \right) \right] \exp \left( \frac{-it}{\eta} \right), \quad (21)$$

$$M_{g3}(t) = \left[ \alpha \left( -1 + \frac{\cos \left( \sqrt{\frac{5}{2}} t \right)}{5} \right) + \alpha i \eta \sqrt{\frac{2}{25}} \left( -1 - \cos \left( \sqrt{\frac{5}{2}} t \right) \right) \right] \exp \left[ \frac{-2it}{\eta} \right], \quad (22)$$

and the three amplitudes are zero:  $M_{e3}(t) = M_{r2}(t) = M_{r3}(t) = 0$ . In Eqs. (14)-(22), the first index  $\sigma$  is located in the atomic states ( $e, r, g$ ), the second index  $m$  is located in the vibrational quantum numbers (0, 1, 2, 3). In the above equations,  $t$  is dimensionless time scaled by  $\nu\eta$ . In Figs. 2, 3, and 4, a scaled time of 6 is equal to 2000 microseconds for LDP=0.3. The calculation is as follows: If  $\eta = 0.3$  and  $\nu = 1 \times 10^4$  Hz, then  $\nu\eta = 3 \times 10^3$ , and the scaled time of 6 is  $(6/\nu\eta) = 2 \times 10^{-3} = 2000$  microseconds. Under the unitary transformation and the interaction picture, we calculated the new general existing state vector as the following:

$$|\psi_{\text{lower}}(t)\rangle = \sum_{n=0}^3 (A_n(t) |e, n\rangle + B_n(t) |r, n\rangle + C_n(t) |g, n\rangle), \quad (23)$$

where  $A_n(t), B_n(t), C_n(t)$  are these amplitudes of the state vector for the TRI-coherent system. Then, the new detailed existing state vector (Eq. 23) is given by

$$\begin{aligned} |\psi_{\text{lower}}(t)\rangle = & A_0 |e, 0\rangle + A_1 |e, 1\rangle + A_2 |e, 2\rangle + A_3 |e, 3\rangle + B_0 |r, 0\rangle \\ & + B_1 |r, 1\rangle + B_2 |r, 2\rangle + B_3 |r, 3\rangle + C_0 |g, 0\rangle + C_1 |g, 1\rangle + C_2 |g, 2\rangle + C_3 |g, 3\rangle. \end{aligned} \quad (24)$$

We denoted the total density operator by  $\rho_{\text{ion-phonon}}$  for a composite quantum state with finite-dimensional Hilbert space. Therefore, we limit the Hilbert space so that the quantum state is easily examined through Eqs. (23-24). The total density operator for three-levels of the TRI interacting with two photons has the form

$$\rho_{\text{ion-phonon}}(t) = |\psi_{\text{lower}}(t)\rangle \langle \psi_{\text{lower}}(t)|. \quad (25)$$

For the new detailed state vector and the density operator of the TRI-coherent system, we use the new notation below:

$$|\psi_{\text{lower}}(t)\rangle = \sum_{n=1}^{12} A_j |e_j\rangle, \quad (26)$$

$$\langle \psi_{\text{lower}}(t)| = \sum_{n=1}^{12} A_l^* \langle e_l| \quad (27)$$

$$\rho_{\text{ion-phonon}} = |\psi_{\text{lower}}(t)\rangle \langle \psi_{\text{lower}}(t)| = \sum_{j=1}^{12} \sum_{l=1}^{12} A_j A_l^* |e_j\rangle \langle e_l|. \quad (28)$$

Here  $|e_1\rangle = |e, 0\rangle, |e_2\rangle = |e, 1\rangle, |e_3\rangle = |e, 2\rangle, |e_4\rangle = |e, 3\rangle, |e_5\rangle = |r, 0\rangle, |e_6\rangle = |r, 1\rangle, |e_7\rangle = |r, 2\rangle, |e_8\rangle = |r, 3\rangle, |e_9\rangle = |g, 0\rangle, |e_{10}\rangle = |g, 1\rangle, |e_{11}\rangle = |g, 2\rangle, |e_{12}\rangle = |g, 3\rangle$  for both  $j$  and  $l$ . After long calculations, these coefficients of the new

detailed state vector are defined as follows:

$$A_c(t) = \frac{1}{\sqrt{2}} e^{-i\omega t/\nu\eta} [M_{rc}(t) + M_{gc}(t)], \quad (c = 0, 1, 2, 3), \quad (29)$$

$$B_0(t) = \left\{ - (1/\sqrt{2}) M_{e_0}(t) - i\eta \left( (1/\sqrt{2}) M_{e_1}(t) + 0.5 M_{g_1}(t) \right) + 0.5 (M_{r_0}(t) - M_{g_0}(t)) \right\}, \quad (30)$$

$$B_1(t) = \left\{ \begin{array}{l} \left\{ - (1/\sqrt{2}) M_{e_0}(t) + 0.5 (M_{r_0}(t) - M_{g_0}(t)) \right\} i\eta - \sqrt{0.5} M_{e_1}(t) \\ + 0.5 (M_{r_1}(t) - M_{g_1}(t)) + i\eta 0.5 \sqrt{2} (M_{r_2}(t) - M_{g_2}(t)) \end{array} \right\}, \quad (31)$$

$$B_2(t) = \left\{ \begin{array}{l} (-M_{e_1}(t) - \sqrt{1.5} M_{e_3}(t) - (0.5) \sqrt{2} M_{g_1}(t)) i\eta \\ + (-\sqrt{0.5} M_{e_2}(t) + (0.5) (M_{r_2}(t) - M_{g_2}(t))) \end{array} \right\}, \quad (32)$$

$$B_3(t) = -0.5 \left( i\eta \sqrt{3} M_{g_2}(t) + M_{g_3}(t) \right), \quad (33)$$

$$C_0(t) = \sqrt{0.5} M_{e_0}(t) + 0.5 (M_{r_0}(t) - M_{g_0}(t)) - i\eta \left( \sqrt{0.5} M_{e_1}(t) - 0.5 M_{g_1}(t) \right), \quad (34)$$

$$C_1(t) = \left\{ \begin{array}{l} i\eta (0.5) \sqrt{2} M_{g_2}(t) - i\eta \left( \sqrt{0.5} M_{e_0}(t) + 0.5 (M_{r_0}(t) - M_{g_0}(t)) \right) \\ + \sqrt{0.5} M_{e_1}(t) + (0.5) (M_{r_1}(t) - M_{g_1}(t)) \end{array} \right\}, \quad (35)$$

$$C_2(t) = -i\eta \sqrt{2} \left( \sqrt{0.5} M_{e_1}(t) - 0.5 M_{g_1}(t) \right) - 0.5 M_{g_2}(t), \quad (36)$$

$$C_3(t) = 0.5 \left( i\eta \sqrt{3} M_{g_2}(t) - M_{g_3}(t) \right), \quad (37)$$

where,  $\omega_{eg}$  is the resonance frequency of e-g levels,  $\omega = \omega_{eg} - \nu\eta^2$ . Four of the 12 coefficients (Eq. 29) are plotted for  $\eta = 0.3$  in Fig. 2. The number of peaks in all plots of Fig. 2 are more numerous than in the remaining eight probability amplitudes.

We showed two the measures of entangled states in Figs. 3, 4 and 5. By quantum mechanical tracing method, we obtained a reduced density operator  $\rho_{\text{ion}} = \text{Tr}_{\text{phonon}}(\rho_{\text{ion-phonon}})$  using Eq. (39). From Eq. (25), the analytic solution of the total density operator becomes

$$\rho_{\text{ion-phonon}} = U^\dagger(t) [\rho^i(0) \otimes \rho^p(0)] U(t). \quad (38)$$

Qudit entangled states can be made observable by measuring quantum entropy [6, 24]. The operator  $\rho_{\text{ion-phonon}}$  is represented by a  $12 \times 12$  matrix. Taking trace over the phonon system,  $3 \times 3$  reduced density operator,  $\rho_{\text{ion}}$  can be written as

$$\rho_{\text{ion}} = \text{Tr}_{\text{phonon}}(\rho_{\text{ion-phonon}}) = \begin{pmatrix} \text{Tr}|e\rangle\langle e| & \text{Tr}|e\rangle\langle r| & \text{Tr}|e\rangle\langle g| \\ \text{Tr}|r\rangle\langle e| & \text{Tr}|r\rangle\langle r| & \text{Tr}|r\rangle\langle g| \\ \text{Tr}|g\rangle\langle e| & \text{Tr}|g\rangle\langle r| & \text{Tr}|g\rangle\langle g| \end{pmatrix}, \quad (39)$$

where diagonal terms,  $|e\rangle\langle e|$ ,  $|r\rangle\langle r|$ , and  $|g\rangle\langle g|$  are these  $4 \times 4$  matrices. The matrix representation of first diagonal term using basis vectors is defined as:

$$|e\rangle\langle e| = \begin{pmatrix} A_0 A_0^* & A_1 A_0^* & A_2 A_0^* & A_3 A_0^* \\ A_0 A_1^* & A_1 A_1^* & A_2 A_1^* & A_3 A_1^* \\ A_0 A_2^* & A_1 A_2^* & A_2 A_2^* & A_3 A_2^* \\ A_0 A_3^* & A_1 A_3^* & A_2 A_3^* & A_3 A_3^* \end{pmatrix}. \quad (40)$$

One of the nine traces in Eq. (39) is defined as:  $\text{Tr}|e\rangle\langle e| = A_0 A_0^* + A_1 A_1^* + A_2 A_2^* + A_3 A_3^*$ . Similarly, other diagonal trace terms can be calculated.

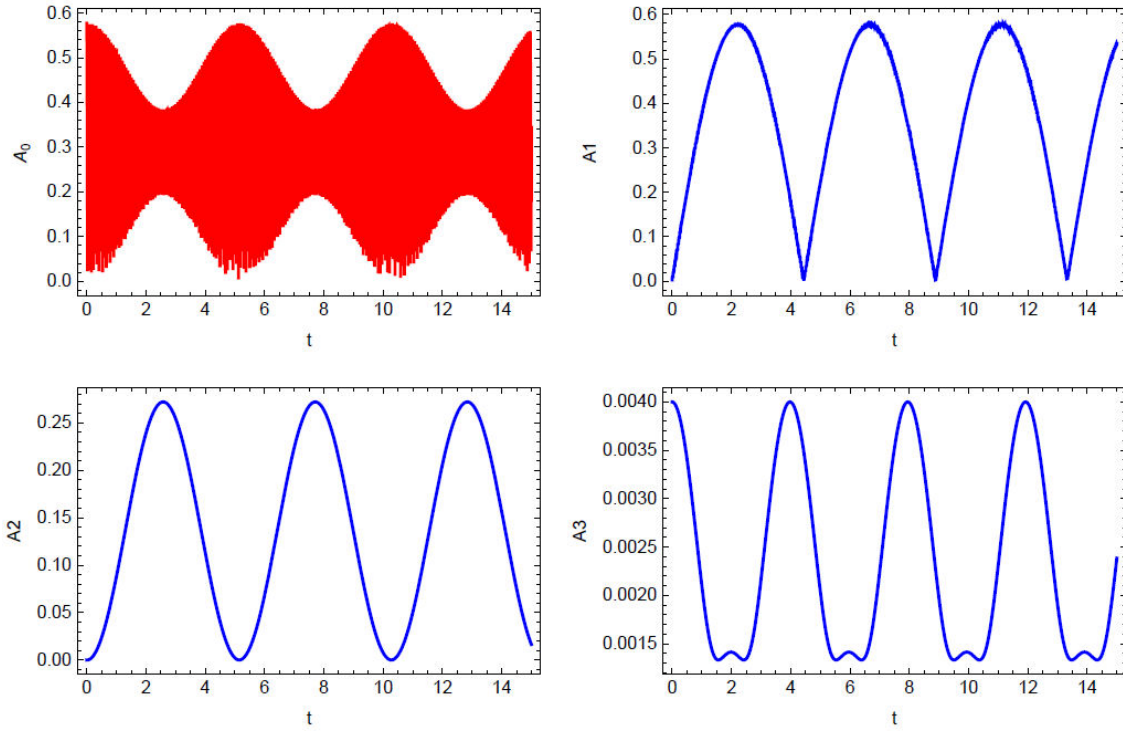


FIGURE 2. Time is dimensionless and scaled by  $\nu\eta$ . Graphs showing the change of  $A_0, A_1, A_2$ , and  $A_3$  coefficients versus scaled time. System's initial state is  $\psi(0) = ([1/\sqrt{3}]|g\rangle + [1/\sqrt{3}]|r\rangle + [1/\sqrt{3}]|e\rangle) \otimes (|0\rangle + \alpha|1\rangle)$  with  $\alpha = 0.005$  and  $\eta = 0.3$ . The linear harmonic trap frequency is  $\nu = 1 \times 10^4$  Hz, the resonance frequency is  $\omega_{eg} = 4 \times 10^{12}$  Hz using the Planck constant equal to one.

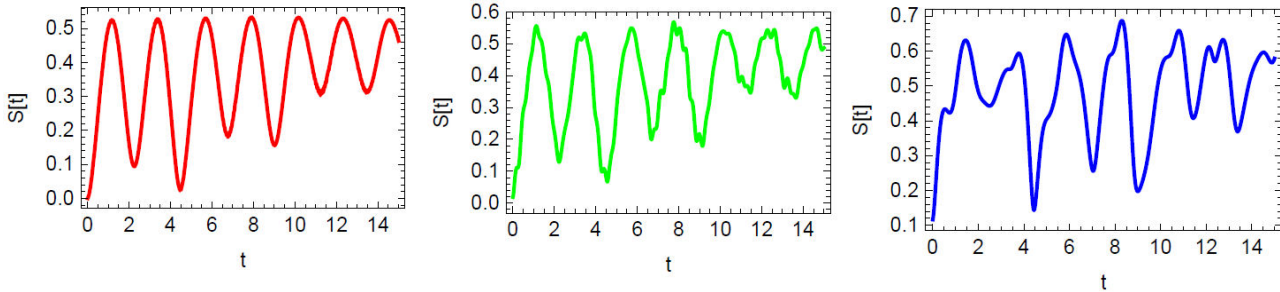


FIGURE 3. The quantum entropy versus scaled time for  $\eta = 0.01, 0.1$ , and  $0.3$ . System's initial state is  $\psi(0) = ([1/\sqrt{3}]|g\rangle + [1/\sqrt{3}]|r\rangle + [1/\sqrt{3}]|e\rangle) \otimes (|0\rangle + \alpha|1\rangle)$ . The other coupling parameters are the same as Fig. 2.

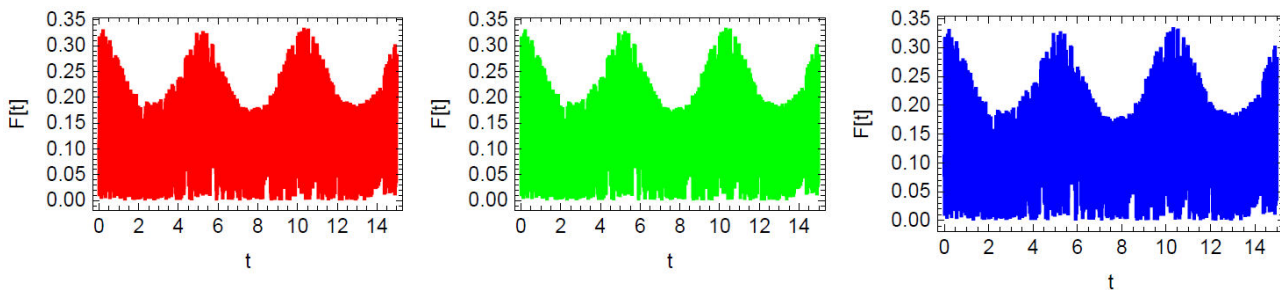


FIGURE 4. The fidelity versus scaled time for  $\eta = 0.01, 0.1$ , and  $0.3$ . The other coupling parameters are the same as Fig. 2.

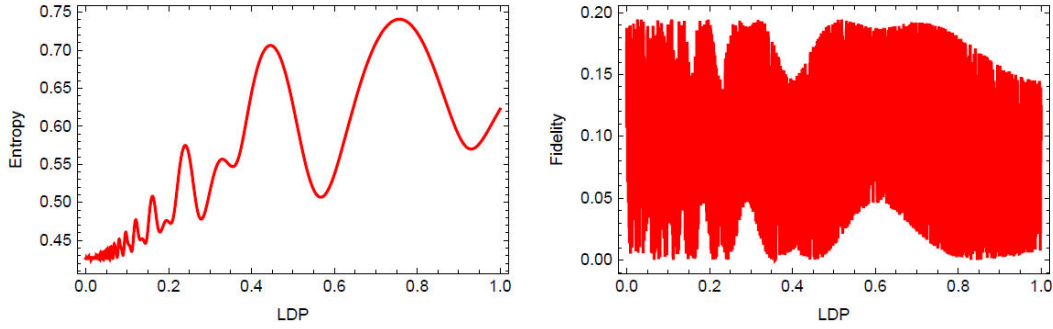


FIGURE 5. The LDP dependence of quantum entropy and fidelity in the two-dimensional graphics. The parameters used are taken as  $\omega_{eg} = 4 \times 10^{12}$  Hz,  $\alpha = 0.005$ ,  $\nu = 1 \times 10^4$  Hz, and the optimum scaled time  $t = 33$  (11.000  $\mu$ s).

### 3. Fidelity, quantum entropy and discussion

It is significant to measure whether there is entanglement in the TRI-coherent system with entropy and fidelity. We investigate the entanglement of the system for values of the LDP between 0.0 and 1.0, according to entropy and fidelity. The internal states of the TRI subsystem are associated with a three-dimensional Hilbert space  $H_i$  of a qutrit spanned by the basis states  $H_i$ . The coherent state subsystem is described by a four-dimensional Hilbert space  $H_p$ . In particular, the Hilbert space of the TRI-coherent system  $H$  is the twelve-dimensional, such as  $H = H_i \otimes H_p = C^3 \otimes C^2 \otimes C^2 = C^3 \otimes C^4 = C^{12}$ . The dimensions of Hilbert space of the system are guides for understanding the density operators. From the new detailed state vector  $|\psi_{lower}(t)\rangle$  (See Eq. 24), the density operator of the TRI-coherent system is shown by  $\rho_{ion-phonon} = |\psi(t)\rangle\langle\psi(t)|$  in Eq. (38). The quantum entropy ( $S$ ) of the TRI-coherent system is defined as in [27]

$$S_{ion}(t) = -Tr_{phonon}[\rho_{ion}\text{Log}(\rho_{ion})] \\ = -[\lambda_1\text{Log}(\lambda_1) + \lambda_2\text{Log}(\lambda_2) + \lambda_3\text{Log}(\lambda_3)], \quad (41)$$

where  $\rho_{ion} = Tr_{phonon}(\rho_{ion-phonon})$  is the reduced density operator in Eq. (39). Entropy can be calculated with three eigenvalues (Schmidt coefficients) of the reduced density operator [21]. The normalization condition of the three eigenvalues is exactly  $\|\lambda_1\| + \|\lambda_2\| + \|\lambda_3\| = 1$ .

In quantum mechanics, especially in quantum information science, fidelity is used to evaluate the transformation between the changing states and the fixed states. With the help of the basic formulas in Ref. [25], we obtained the fidelity of the system as follow: [28, 29]

$$F(t) = \sqrt{\langle\psi(0)|\hat{\rho}(t)|\psi(0)\rangle} = \langle\psi(0)|\psi(t)\rangle \\ = \frac{1}{\sqrt{3}}[A_0(t) + \alpha^*A_1(t) + B_0(t) \\ + \alpha^*B_1(t) + C_0(t) + \alpha^*C_1(t)] \quad (42)$$

where  $|\psi(t)\rangle$  is given by Eq. (24) and  $|\psi(0)\rangle$  is given by Eq. (12).

We focus on the quantum dynamics and the quantum correlations of two quantum measures with figures. The entropy

in Fig. 3 and the fidelity in Fig. 4 are obtained for three different LDPs. These three values of LDP are within the deep LD regime is qualified by a small  $\eta = 0.01$  or  $\eta = 0.3$ ; on the other hand, beyond the LD regime is  $\eta = 0.4$  [20]. The fidelity is certainly recorded  $F = 0.34$  at the peak for  $\eta = 0.1$  in Fig. 4. The scaled optimum time (scaled time=33, 11.000 ns) was found with this research, by evaluating in Figs. 3 and 4. These findings are consistent with the findings obtained in previous studies [19, 21, 25]. We can see in Fig. 3 that the entanglement values increase with the rise of LDP. If Fig. 5 and these results are evaluated together, the experimental limit for fidelity is compatible with LDP = 1.0 via Eq. (42) [28].

Figure 5 appears that the entropy (left panel) rather than fidelity (right panel) allows more entanglement lifetime. We demonstrated quantum entanglement with entropy in the deep LD regime distinctively in Ref. [21]. In this graph, as LDP grows the entropy increases, which means that the entangled lifetime is raising. For example, the state of the TRI-coherent system is disentangled at scaled time 18,  $t = 6.000 \mu$ s for  $\eta = 0.3$ . The system reaches a local minimum which corresponds to a separable quantum state

$$|\psi(t = 18)\rangle = (0.623|r\rangle + 0.52|g\rangle + 0.61|e\rangle) \otimes |0\rangle. \quad (43)$$

Similarly the state of the TRI-coherent system is maximally entangled at scaled time 33,  $t = 11.000 \mu$ s for  $\eta = 0.3$ . We get a local maximum which corresponds to a partially quantum state

$$|\psi(t = 33)\rangle = (0.51|r\rangle + 0.42|g\rangle + 0.43|e\rangle) \otimes |0\rangle \\ + (0.471|e\rangle + 0.22|r\rangle + 0.31|g\rangle) \otimes |1\rangle \\ + (0.1|r\rangle + 0.1|g\rangle) \otimes |2\rangle. \quad (44)$$

The optimum time to reach an arbitrary entangled state is 11.000 ns (scaled time 33); see Fig. 5. In line with of the measures and the results reported above, we observed that the maximally entangled states do not collapse in the TRI-coherent system. We examined with  $S$  that the measurement degrees have a sudden appearance of the entangled state in parallel with raising  $\eta$ , which is in agreement with previous

observations [21, 28–30]. The article in Ref. [31] characterized the application of Schmidt mode analysis for pure states.

#### 4. Concluding remarks

In this paper, we examined whether the full TRI-coherent system with a harmonic trap frequency of  $10^4$  Hz is entangled or not. We analyzed the quantum correlations of the system via three coupling parameters ( $\eta$ ,  $\nu$  and  $\Omega$ ). After that, we discovered that for  $\eta = 0.3$  it survives longer than for  $\eta = 0.1$  and  $\eta = 0.01$ . This observation demonstrates that entangled states are directly connected with the LDP. We show a high degree of the quantum entanglement of the full TRI-coherent system using two elaborated measures of the family consisting of  $S$  and  $F$ . The entropy behavior is similar to the fidelity behavior when we change the LDP. Comparing three graphs in the Fig. 3, we determined that entangled states are stored in the TRI-coherent system. Besides, the amount of entanglement has two maximum values for  $S = 0.68$  and  $F = 0.35$  in  $\eta = 0.3$ . Also, the first graph of Fig. 3 shows that the system's entropy is described by a Gaussian-like profile as a function of scaled time.

Our results can be helpful in engineering the science of entanglement. The quantum correlations yielded the following significant developments in this study.

- (1)  $\sqrt{1/3}$  is taken the three probability amplitudes of the TRI, based on the analytic solution for the new existing state vector. Then, the full TRI has been achieved with

these probability amplitude values. The total density and the reduced density operators of the new existing state vector are calculated theoretically in this study.

- (2) In the right panel of Fig. 5, it can be easily seen that the amount of fidelity increases when the LDP increases. In the left panel of Fig. 5, we have shown that the lifetime of entropy, namely, entanglement, also increased when the LDP increased.
- (3) Figure 3 and the left panel of Fig. 5 have been plotted using three eigenvalues of the reduced density matrix, called Schmidt coefficients.

In summary, the  $S$  measurement indicates the length of life of entanglement, while  $F$  indicates the maximally entangled state. The long-lived and maximally entangled states presented in this study can serve as a guide to researchers trying to add innovative aspects to the science of entanglement.

#### Acknowledgments

We thank to Özgür E Müstecaplıoğlu, Burak Avsar and Seref K. Tellioglu for fruitful discussions. The authors are grateful to the referees for their constructive criticisms and advices. This work was supported by Afyon Kocatepe University 09-FENED.06 project in Türkiye. The English language of this study is edited separately by Grammarly and the English editing company, Lexicon-Türkiye.

- 
1. A. Einstein, B. Podolsky, N. Rosen, *Can quantum-mechanical description of physical reality be considered complete?*, Phys. Rev. **47** (1935) 777, <https://link.aps.org/doi/10.1103/PhysRev.47.777>.
  2. E. Schrödinger, *Die gegenwärtige Situation in der Quantenmechanik*, Naturwissenschaften **23** (1935) 807, <https://doi.org/10.1007/BF01491891>.
  3. N. Bohr, *Can quantum-mechanical description of physical reality be considered complete?*, Phys. Rev. **48** (1935) 696, <https://doi.org/10.1103/PhysRev.48.696>.
  4. C. Quintana and O. Rosas-Ortiz, *Note on the quantum correlations of two qubits coupled to photon baths*, J. Phys.: Conf. Ser. **624** (2015) 012004, <https://doi.org/10.1088/1742-6596/624/1/012004>.
  5. D. Leibfried, R. Blatt, C. Monroe, D. Wineland, *Quantum dynamics of single trapped ions*, Phys. Rev. Mod. **75** (2003) 281, <https://doi.org/10.1103/RevModPhys.75.281>.
  6. M. Abdel-Aty, *Manipulating mixed state entanglement between a time-dependent field and a three-level trapped ion*, Optics Comm. **266** (2006) 225, <https://doi.org/10.1016/j.optcom.2006.04.060>.
  7. M. Bock, P. Eich, S. Kucera, et al., *High-fidelity entanglement between a trapped ion and a telecom photon via quantum frequency conversion*, Nat. Commun. **9** (2018) 1998, <https://doi.org/10.1038/s41467-018-04341-2>.
  8. C. Brukner, M. Zukowski, A. Zeilinger, *Quantum Communication Complexity Protocol with Two Entangled Qubits*, Phys. Rev. Lett. **89** (2002) 197901, <https://doi.org/10.1103/PhysRevLett.89.197901>.
  9. R. Dermez, *Quantifying of quantum entanglement in Schrödinger cat states with the trapped ion-coherent system for the deep Lamb-Dick regime*, Indian J. Phys. **95** (2021) 219, <https://doi.org/10.1007/s12648-020-01697-4>.
  10. R. Dermez, *Quantification of Mixed-State Entanglement in a Quantum System Interacting with Two Time-Dependent Lasers*, J. Russ. Laser Res. **34** (2013) 192, <https://doi.org/10.1007/s10946-013-9342-y>.
  11. P. A. M. Dirac, *The Principles of Quantum Mechanics*, Clarendon, Oxford, 4th edition, (1930) 1995.
  12. R. Jozsa, *Fidelity for Mixed Quantum States*, Journal of Modern Optics **41** (1993) 2315, <https://doi.org/10.1080/09500349414552171>.
  13. A. Uhlmann, *Fidelity and concurrence of conjugated states*, Phys. Rev. A **62** (2000) 032307, <https://doi.org/10.1103/PhysRevA.62.032307>.

14. A. Uhlmann, *The transition probability in the state space of a \*-algebra*, Report on Math. Physics **9** (1976) 273, [https://doi.org/10.1016/0034-4877\(76\)90060-4](https://doi.org/10.1016/0034-4877(76)90060-4).
15. W. K. Wootters, *Entanglement of Formation of an Arbitrary State of Two Qubits*, Phys. Rev. Lett. **80** (1998) 2245, <https://doi.org/10.1103/PhysRevLett.80.2245>.
16. S. Nandi, C. Datta, A. Das, P. Agrawal, *Two-qubit mixed states and teleportation fidelity: purity, concurrence, and beyond*, Eur. Phys. J. D **72** (2018) 182, <https://doi.org/10.1140/epjd/e2018-90252-2>.
17. P. Kobel, M. Breyer, M. Kohl, *Deterministic spin-photon entanglement from a trapped ion in a fiber Fabry-Perot cavity*, npj Quantum Inf. **7** (2021) 6, <https://doi.org/10.1038/s41534-020-00338-2>.
18. Y. Lee, E. Bersin, A. Dahlberg, S. Wehner, D. Englund, *Hybrid Quantum Networks for High-Fidelity Entanglement Distribution*, OSA Technical Digest (Optical Society of America) in Conference on Lasers and Electro-Optics, 2020, <https://doi.org/10.1364/CLEO-QELS.2020.FTh3D.5>.
19. S.J. Anvar, M. Ramzan, M.K. Khan, *Dynamics of entanglement and quantum Fisher information for N-level atomic system under intrinsic decoherence*, Quantum Inf. Process **16** (2017) 142, <https://doi.org/10.1007/s11128-017-1589-8>.
20. Ö. E. Müstecaplıoğlu, *Motional macroscopic quantum superposition states of a trapped three-level ion*, Phys. Rev. A **68** (2003) 023811, <https://doi.org/10.1103/PhysRevA.68.023811>.
21. R. Dermez, B. Deveci and D. Ö. Güney, *Quantum dynamics of a three-level trapped ion under a time-dependent interaction with laser beams*, Eur. Phys. J. D **67** (2013) 120 <https://doi.org/10.1140/epjd/e2013-30649-9>.
22. C. Crocker, M. Lichtman, K. Sosnova, A. Carter, S. Scarano, C. Monroe, *High purity single photons entangled with an atomic qubit*, Opt. Express **27** (2019) 28143, <https://doi.org/10.1364/OE.27.028143>.
23. M. Um, J. Zhang, D. Lv, et al., *Phonon arithmetic in a trapped ion system*, Nat. Commun. **7** (2016) 11410, <https://doi.org/10.1038/ncomms11410>.
24. N. Grzesiak, R. Blümel, et al., *Efficient arbitrary simultaneously entangling gates on a trapped-ion quantum computer*, Nature Communications **11** (2020) 2963, <https://doi.org/10.1038/s41467-020-16790-9>.
25. R. Dermez, S. Abdel-Khalek, E. M. Khalil, *Fidelity and concurrence of entangled qudits between a trapped ion and two laser beams*, Rev. Mex. Fis. **67** (2021) 050705, <https://doi.org/10.31349/RevMexFis.67.050705>.
26. J.J. Sakurai, *Modern Quantum Mechanics*, Addison-Wesley Publishing Company (1994).
27. J. von Neumann, *Mathematical Foundations of Quantum Mechanics* (Princeton, NJ: Princeton University Press) (1995).
28. J.-X. Wang, X.-J. Zhang and X.-X. Zhang, *Evolution Properties of Atomic Fidelity in the Combined Multi-Atom-Cavity Field System*, Commun. Theor. Phys. **63** (2015) 749, <https://doi.org/10.1088/0253-6102/63/6/749>.
29. S. V. Prants, M. Yu. Uleysky and V. Yu. Argonov, *Entanglement, fidelity, and quantum-classical correlations with an atom moving in a quantized cavity field*, Phys. Rev. A **73** (2006) 023807, <https://doi.org/10.1103/PhysRevA.73.023807>.
30. R. Dermez, Y. Tunçer, *Eskisehir Technical University Journal of Science and Technology B-Theoretical Science* **8**(2), 316 (2020), <https://doi.org/10.20290/estubtdb.706641>.
31. J.H. Eberly, *Schmidt analysis of pure-state entanglement*, Laser Phys. **16** (2006) 921, <https://doi.org/10.1134/S1054660X06060041>.